

Chapter 26

Thermodynamics of Fuel Cells

26.1 Fuel Cells

We have seen before that entropy generation in combustion, and subsequent heat transfer, leads to considerable irreversible work losses. The combustion loss can be attributed to the uncontrolled movement of electrons as new molecules are formed in the reaction. Fuel cells offer a process in which the electron movement is controlled, and thus no combustion losses occur. The performance of real life fuel cells is diminished by irreversible losses due to resistance, reaction activation and mass flow restrictions, and these will be discussed after the basic discussion of fuel cells and their efficiencies.

In fuel cells an electrochemical process allows to directly convert the energy stored in a fuel into electrical energy. There are many types of fuel cells that consume different fuels, e.g. direct methanol fuel cells, direct carbon fuel cells, and hydrogen fuel cells. Large parts of the discussion below are valid for all types, however, when it comes to evaluation of the equations, we shall consider only hydrogen fuel cells with the overall reaction



Figure 26.1 shows a schematic of a hydrogen fuel cell. Hydrogen and oxygen (pure or with air) are supplied to the two sides of the fuel cell in transport channels, and enter gas diffusion layers (GDL) through which they travel towards the catalyst layer. The GDL shields the gas from the electrolyte, and contributes to the management of water flows within the cell. The electrochemical reactions take place in the catalyst layers at anode and cathode. These are separated by an electrolyte through which electrons cannot pass. The electrons move from anode to cathode through the electrical device (with resistance R_d) and provide the power \dot{W} to run the device. At the same time ions move through the electrolyte.

The reactions at anode and cathode, and the transport processes through the electrolyte depend on the type of electrolyte.

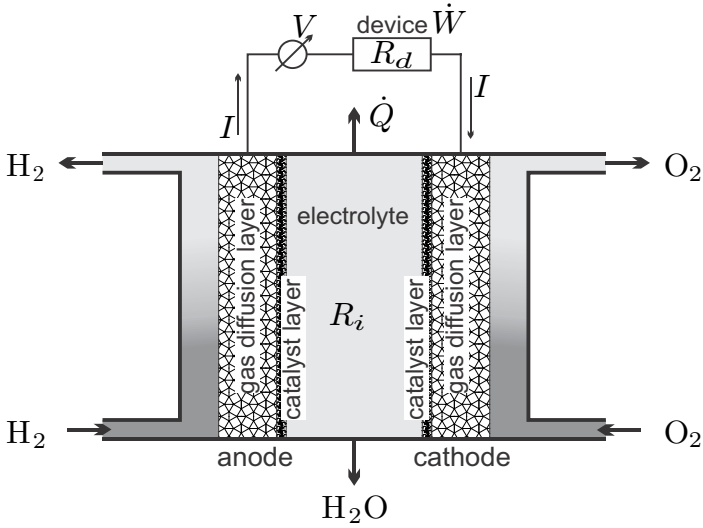


Fig. 26.1 Schematic of a fuel cell

Figure 26.2 sketches the reactions for an acidic electrolyte, e.g., phosphoric acid ($\text{PO}_4^{3-} + 3\text{H}^+$ + water), or polyelectrolyte membranes (PEM), which are polymers with sulfuric acid groups (polymer + $\text{SO}_3^- + \text{H}^+$ + water). At the anode, the incoming hydrogen is split into electrons, e^- , and protons, H^+ . The protons travel through the electrolyte to the cathode, while the electrons pass through the device. At the cathode, protons, electrons and the incoming oxygen react to water, which must be removed from the electrolyte.

In alkaline electrolyte fuel cells, see Fig. 26.3, the electrolyte is a base, e.g., potassium hydroxide ($\text{K}^+ + \text{OH}^-$ + water). At the anode, the incoming hydrogen reacts with hydroxide, OH^- , to form water and electrons, which travel through the electrical device to the cathode. At the cathode, the electrons and the incoming oxygen react with water to form hydroxide, that then travels through the electrolyte to the anode, while half of the water produced at the anode travels through the electrolyte to replenish the water consumed in the cathode reaction.

In both types of fuel cells, the ion and electron movement is forced by the electric potential V between cathode and anode.

26.2 Fuel Cell Potential

For the thermodynamic analysis of fuel cells, it is not necessary to distinguish between acidic and alkaline fuel cells. We consider the mass and energy flows as in Fig. 26.1, and apply the first and second law, which read for steady state operation

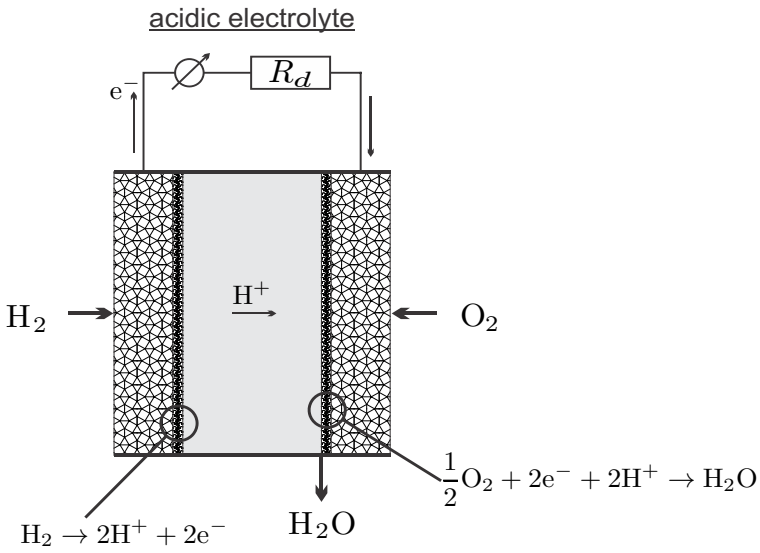


Fig. 26.2 Acidic electrolyte fuel cell

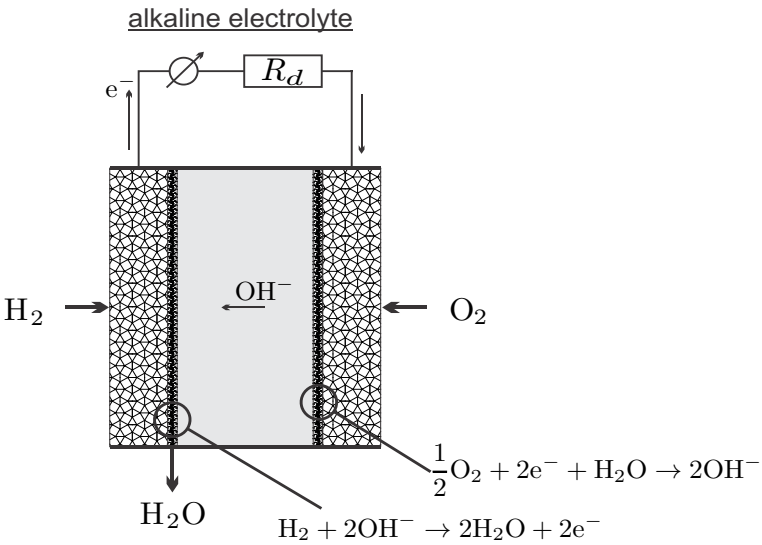


Fig. 26.3 Alkaline electrolyte fuel cell

$$\sum_{\alpha, out} \dot{n}_\alpha \bar{h}_\alpha - \sum_{\alpha, in} \dot{n}_\alpha \bar{h}_\alpha = \dot{Q} - \dot{W} , \quad (26.2)$$

$$\sum_{\alpha, out} \dot{n}_\alpha \bar{s}_\alpha - \sum_{\alpha, in} \dot{n}_\alpha \bar{s}_\alpha - \frac{\dot{Q}}{T} = \dot{S}_{gen} \geq 0 . \quad (26.3)$$

For most of our discussion, the system to be considered is just the fuel cell. For the evaluation we shall assume that all inflows and outflows take place at the homogeneous fuel cell temperature T . Additional irreversible processes (external losses) might occur outside the fuel cell, e.g., in the heating of the incoming oxygen and hydrogen, or in the heat transfer \dot{Q} between the fuel cell and its exterior environment.

Combining the two laws by elimination of the heat \dot{Q} yields

$$\dot{W} = \sum_{\alpha, in} \dot{n}_\alpha \bar{g}_\alpha - \sum_{\alpha, out} \dot{n}_\alpha \bar{g}_\alpha - T \dot{S}_{gen} . \quad (26.4)$$

In order to guarantee sufficient supply of fuel and oxidizer to the gas diffusion layers at all locations along the gas channels, one normally will have excess hydrogen and oxygen which are circulated back to the inlet (at least the hydrogen).

The rate of reactions taking place is denoted by Λ so that the incoming and outgoing mole flows are related to the reaction rate by

$$\dot{n}_{\text{H}_2}^{in} - \dot{n}_{\text{H}_2}^{out} = \Lambda \quad , \quad \dot{n}_{\text{O}_2}^{in} - \dot{n}_{\text{O}_2}^{out} = \frac{1}{2} \Lambda \quad , \quad \dot{n}_{\text{H}_2\text{O}}^{out} = \Lambda . \quad (26.5)$$

For each reaction there are two electrons traveling through the electrical device which corresponds to the electrical current

$$I = 2F\Lambda . \quad (26.6)$$

Here $F = 96485 \frac{\text{Cb}}{\text{mol}}$ denotes Faraday's constant (Michael Faraday, 1791-1867), which gives the absolute value of the electrical charge per mole of electrons.

The electrical power consumed by the external device is $\dot{W} = VI = R_d I^2$ and thus, with $\Lambda = \frac{I}{2F}$,

$$\dot{W} = VI = -\frac{I}{2F} \Delta \bar{g}_R - T \dot{S}_{gen} , \quad (26.7)$$

where $\Delta \bar{g}_R$ is the Gibbs free energy of reaction at T . The fuel cell potential follows as

$$V = -\frac{\Delta \bar{g}_R}{2F} - \frac{T \dot{S}_{gen}}{I} . \quad (26.8)$$

The last term, $\frac{T \dot{S}_{gen}}{I} = V_{\text{over}}$ is the overpotential, i.e., the potential loss due to irreversible processes within the fuel cell. In Section 25.11 it was shown

that the Gibbs free energy of reaction is the maximum amount of work that can be obtained per mole of fuel. This work could be obtained from a fully reversible fuel cell, where $V_{\text{over}} = 0$.

When the electron circuit is interrupted, reactions cannot take place, and accordingly no irreversible processes occur. In this case one measures the open circuit voltage between anode and cathode,¹

$$V_0 = -\frac{\Delta\bar{g}_R}{2F}. \quad (26.9)$$

At standard reference conditions, the open circuit potential of a hydrogen fuel cell is $V_0 = 1.23V$. Higher voltages, and thus higher powers, are obtained by connecting several cells in series, to form fuel cell stacks.

26.3 Fuel Cell Efficiency

Efficiencies of engines are normally defined as

$$\eta = \frac{\text{gain}}{\text{expense}}, \quad (26.10)$$

where for power producing heat engines the gain is the power produced, and the expense is the heat put into the engine through the combustion of fuel, nuclear reactions, etc. Fuel cells are not heat engines, and thus the question arises how to best define their efficiency. The gain is the power produced, hence this is a question of defining the expense.

For comparison of heat engines and fuel cells the following definition is often used: In a combustion process one could obtain the heat $\dot{Q}_C = -\Lambda\Delta\bar{h}_R = -\frac{I}{2F}\Delta\bar{h}_R$. Considering this heat as the expense, one defines the “thermal efficiency” of a fuel cell as

$$\eta_{\text{th}}^{\text{FC}} = \frac{\dot{W}}{\dot{Q}_C} = \frac{-\Delta\bar{g}_R - \frac{2F}{I}T\dot{S}_{\text{gen}}}{-\Delta\bar{h}_R}. \quad (26.11)$$

With this definition, the perfect—i.e., reversible—fuel cell has the efficiency

$$\eta_{\text{th}}^{\text{FC}} = \frac{-\Delta\bar{g}_R}{-\Delta\bar{h}_R} = \frac{-(\Delta\bar{h}_R - T\Delta\bar{s}_R)}{-\Delta\bar{h}_R} = 1 - \frac{T\Delta\bar{s}_R}{\Delta\bar{h}_R}. \quad (26.12)$$

For all fuels $\Delta\bar{h}_R < 0$, but there is no definite sign for the entropy of reaction $\Delta\bar{s}_R$. For the hydrogen reaction, $\Delta\bar{s}_R < 0$ and thus $\eta_{\text{th}}^{\text{FC}} < 1$ for reversible fuel cells (irreversible fuel cells have even smaller efficiencies, of course). However, there are reactions, in particular the reaction between carbon and oxygen, $\text{C} + \text{O}_2 \rightleftharpoons \text{CO}_2$, in direct carbon fuel cells, for which the entropy of reaction

¹ There is no current, so that $I = 0$ and $\dot{W} = 0$.

is positive, $\Delta\bar{s}_R > 0$, so that $\eta_{\text{th}}^{\text{FC}}$ as given in (26.11) becomes larger than unity. A proper efficiency measure should always assume values between zero and unity. It follows that the efficiency definition (26.11) is not suitable for the evaluation of fuel cells.

In order to understand why this efficiency measure can be above unity, one needs to consider that, according to the second law, the heat exchanged with the surroundings for the reversible fuel cell is $T\Delta\bar{s}_R$. If $T\Delta\bar{s}_R < 0$, heat is rejected into the surroundings, but if $T\Delta\bar{s}_R > 0$, heat is imported from the surroundings.

One should not be surprised that this efficiency definition leads to problems, since the heat of reaction, $-\Delta\bar{h}_R$, is not relevant in the thermodynamics of fuel cells, as is apparent in that it does not appear in the discussion of fuel cell power and voltage. Heat of reaction is a quantity relevant only for combustion systems.

A more meaningful efficiency is the ratio of the actual power produced by the fuel cell and the maximum power that could be obtained from the fuel, in a fully reversible process. This leads to the second law efficiency,

$$\eta_{FC}^{\text{II}} = \frac{\dot{W}}{\dot{W}_{\text{rev}}} = \frac{V}{V_0} = 1 - \frac{T\dot{S}_{\text{gen}}}{(-\Delta\bar{g}_R)\frac{I}{2F}}, \quad (26.13)$$

which is always positive, and becomes unity only when all irreversibilities vanish.

When only the fuel cell is considered, $\Delta\bar{g}_R$ is to be evaluated at the fuel cell temperature T . The following table shows the Gibbs free energy, the open circuit voltage V_0 , and the ratio $\frac{-\Delta\bar{g}_R}{-\Delta\bar{h}_R}$ of the hydrogen fuel cell as a function of temperature (product water is liquid for $T = 25^\circ\text{C}, 80^\circ\text{C}$ and vapor for higher temperatures²) at standard pressure p_0 :

T	$-\Delta\bar{g}_R$	$V_0 = \frac{-\Delta\bar{g}_R}{2F}$	$\frac{-\Delta\bar{g}_R}{-\Delta\bar{h}_R}$
25 °C	237.2 $\frac{\text{kJ}}{\text{mol}}$	1.23 V	0.83
80 °C	228.2 $\frac{\text{kJ}}{\text{mol}}$	1.18 V	0.80
100 °C	225.2 $\frac{\text{kJ}}{\text{mol}}$	1.17 V	0.79
200 °C	220.4 $\frac{\text{kJ}}{\text{mol}}$	1.14 V	0.77
400 °C	210.3 $\frac{\text{kJ}}{\text{mol}}$	1.09 V	0.74
600 °C	199.6 $\frac{\text{kJ}}{\text{mol}}$	1.04 V	0.70
800 °C	188.6 $\frac{\text{kJ}}{\text{mol}}$	0.98 V	0.66
1000 °C	177.6 $\frac{\text{kJ}}{\text{mol}}$	0.92 V	0.62

All three quantities decrease with increasing temperature. Thus, if one considers a fuel cell alone, one will gain more work at lower temperatures. High temperature fuel cells, e.g. solid oxide fuel cells, operate at temperatures between 700 and 1000 °C, and thus have lower open circuit voltages than low

² For the Gibbs free enthalpy, this makes no difference!

temperature fuel cells. However, due to the high temperatures, the activation losses (see below) are lower, and expensive catalysts are not required. Moreover, the heat rejected from high temperature fuel cells can be used to drive heat engines in a combined cycle to produce additional power. If the heat is barely rejected into the environment, there is an external loss.

In other words, fuel cells must be imbedded into a system, where the fuel cell is at the center, but additional systems for extracting work, heating and cooling must be considered as well. In order to clarify this, Fig. 26.4 shows a (reversible) fuel cell operating at temperature T as part of a fully reversible external system, where the incoming fuel and oxidizer are heated to T by a series of infinitesimal Carnot heat pumps, the heat \dot{Q}_{FC} rejected from the fuel cell drives a Carnot heat engine, and the exhaust is cooled through infinitesimal Carnot heat engines so that it leaves at T_0 . Of course, other fully reversible set-ups are possible, e.g., some heat could be exchanged between the incoming reactant streams and the product stream, using reversible counter-flow heat exchangers. Heat is only exchanged at environmental temperature, and since all incoming and outgoing mass flows are at T_0 and since the system exchanges heat only at T_0 , and when all flows are at p_0 , the work produced per mole of fuel is given by (25.18),

$$\dot{W}_{rev} = \dot{W}_{FC} + \dot{W}_C = -\dot{n}_{fuel} \Delta \bar{g}_R(T_0, p_0) = -\frac{I}{2F} \Delta \bar{g}_R(T_0, p_0) . \quad (26.14)$$

Thus, the obvious definition of a second law efficiency for a fuel consuming system is the relative amount of the work that is actually produced from the available work, i.e.,

$$\eta_{system}^{II} = \frac{\dot{W}}{\dot{W}_{rev}} = 1 - \frac{T_0 \dot{S}_{gen}}{\dot{W}_{rev}} = 1 - \frac{T_0 \dot{S}_{gen}}{-\dot{n}_{fuel} \Delta \bar{g}_R(T_0, p_0)} . \quad (26.15)$$

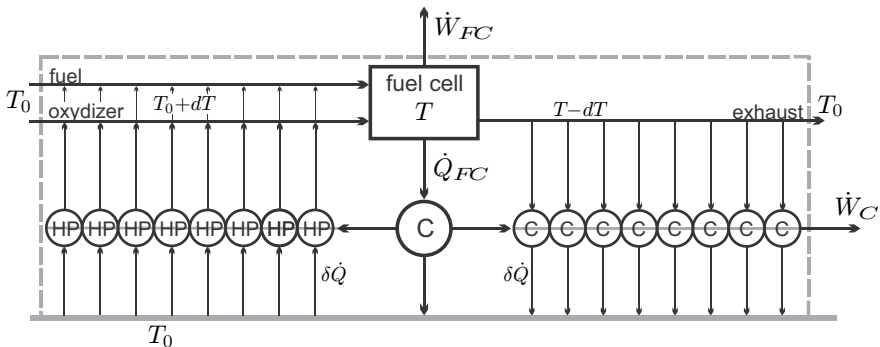


Fig. 26.4 Fuel cell embedded into a fully reversible system of Carnot heat engines and Carnot heat pumps. Heat is only exchanged at environmental temperature T_0 .

This definition can be used for the evaluation of *any* fuel consuming power generation device that is embedded in the environmental at T_0 . The relation between the second law efficiency and the thermal efficiency is

$$\eta_{\text{system}}^{\text{II}} = \frac{\dot{W}}{\dot{W}_{\text{rev}}} = \frac{\dot{W}}{\dot{Q}_C} \frac{\dot{Q}_C}{\dot{W}_{\text{rev}}} = \eta_{\text{th}} \eta_{\text{heat}} \frac{\Delta \bar{h}_R(T_0, p_0)}{\Delta \bar{g}_R(T_0, p_0)}. \quad (26.16)$$

Here we introduced the heat utilization factor

$$\eta_{\text{heat}} = \frac{\dot{Q}_C}{-\dot{n}_{\text{fuel}} \Delta \bar{h}_R(T_0, p_0)} \quad (26.17)$$

to account for losses in heat exchanger and exhaust; \dot{Q}_C is the heat actually transmitted into the heat engine, while $-\Delta \bar{h}_R$ is the available heat.

To finish this section we present and criticize a misleading figure that is sometimes found in the fuel cell literature. Figure 26.5 shows the thermal efficiency (26.11) of a reversible hydrogen fuel cell, $\eta_{\text{th}}^{\text{FC}} = \frac{\Delta \bar{g}_R(T)}{\Delta \bar{h}_R(T)}$, and the efficiency of a Carnot heat engine, $\eta_C = 1 - \frac{T_0}{T}$, both plotted over temperature T . The Carnot efficiency η_C grows with temperature, while $\frac{\Delta \bar{g}_R(T)}{\Delta \bar{h}_R(T)}$ decreases. The figure seems to imply that at higher temperatures fuel cell efficiency might not be as good as the efficiency of a heat engine.

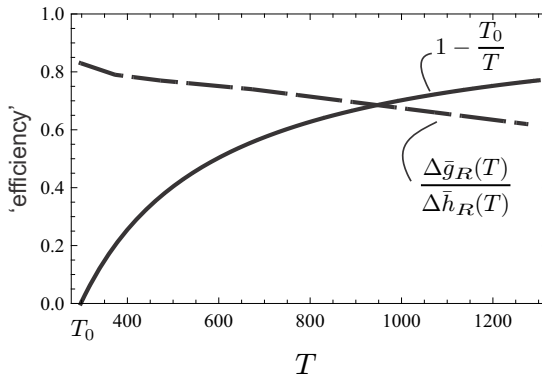


Fig. 26.5 A misleading figure ... see the discussion in the text

This interpretation is misleading for two reasons: (a) As discussed above, a high temperature fuel cell must be seen as one element in a larger system that includes heat engines to convert the high temperature heat rejected from the fuel cell and its exhaust. (b) The Carnot efficiency is relevant only for heat engines operating between two reservoirs at constant temperatures T, T_0 . A heat engine that is driven by the reaction of a fuel does not belong into that category, and thus the Carnot efficiency is not necessarily relevant for a fuel driven engine process.

The proper efficiency measure to compare fuel cell systems and heat engines is the second law efficiency $\eta_{\text{system}}^{\text{II}}$, Eq. (26.15), which relates the actual work produced to the maximum amount that could be produced in a fully reversible process. For real engines, this efficiency is below unity, due to entropy generation in irreversible processes. As discussed in Sec. 25.12, combustion engines suffer from losses in combustion, heat transfer, friction and mixing. Fuel cells suffer from a different array of irreversible losses that will be discussed below. Whether or not a fuel cell system will have a higher efficiency than a combustion system depends on the details of the design, materials used, and the processes within the *system*.

26.4 Nernst Equation

The Nernst equation describes how the Gibbs free energy of reaction, and thus open circuit voltage and power generation of a fuel cell, depends on the pressures of the reactant and product streams. Indeed, so far we have only considered the temperature dependence of $\Delta\bar{g}_R$ and implicitly assumed that the flows are at reference pressure. Now we consider the more general case, where the in- and outflows have different pressures p_α .

To simplify the argument, we assume that all streams are ideal gases, so that $\bar{s}_\alpha(T, p_\alpha) = \bar{s}_\alpha^0(T) - \bar{R} \ln \frac{p_\alpha}{p_0}$. As always, $\bar{s}_\alpha^0(T)$ is the tabulated entropy at reference pressure p_0 . We recall the definitions $\Delta\bar{g}_R = \Delta\bar{h}_R - T\Delta\bar{s}_R$ with $\Delta\bar{h}_R = \sum_\alpha \gamma_\alpha \bar{h}_\alpha(T)$ and $\Delta\bar{s}_R = \sum_\alpha \gamma_\alpha \bar{s}_\alpha(T, p_\alpha)$. This gives the Nernst equation

$$\Delta\bar{g}_R(T, p_\alpha) = \Delta\bar{g}_R(T, p_0) + \bar{R}T \ln \prod_\alpha \left(\frac{p_\alpha}{p_0} \right)^{\gamma_\alpha}, \quad (26.18)$$

where the argument (T, p_α) indicates that the in- and outflows are all at the same temperature T , but at different pressures p_α .

For a hydrogen fuel cell in which the product is steam, the Nernst equation gives the open circuit potential

$$V_0 = \frac{1}{2F} \left[-\Delta\bar{g}_R(T, p_0) + \bar{R}T \ln \frac{p_{\text{H}_2} \sqrt{p_{\text{O}_2}}}{p_{\text{H}_2\text{O}} \sqrt{p_0}} \right]. \quad (26.19)$$

If the product water is liquid, the entropy of the water is independent of pressure due to incompressibility, $\bar{s}_{\text{H}_2\text{O}}(T, p_{\text{H}_2\text{O}}) = \bar{s}_{\text{H}_2\text{O}}(T)$, and the open circuit potential is

$$V_0 = \frac{1}{2F} \left[-\Delta\bar{g}_R(T, p_0) + \bar{R}T \ln \frac{p_{\text{H}_2} \sqrt{p_{\text{O}_2}}}{\sqrt{p_0^3}} \right]. \quad (26.20)$$

These two equations show that the open circuit voltage can be increased by supplying fuel (H_2) and oxidizer (O_2) at elevated pressures. When the product is steam, lowering the steam pressure increases the open circuit voltage.

26.5 Mass Transfer Losses

The pressure considered in the Nernst equation above are the pressures at which the inflows are supplied, and the outflows are removed, that is the pressures in the transport channels. The transport of reactants and products through the porous gas diffusion layers leads to friction losses, and thus generation of entropy as discussed in Sec. 9.7. Entropy generation and overpotential associated with this loss will be determined next.

The flow through the porous medium can be described by Darcy’s law (9.30) which we can write for mole flows as

$$\dot{n}_\alpha = K (p_{\alpha,1} - p_{\alpha,2}) , \tag{26.21}$$

where flow goes from $p_{\alpha,1}$ to $p_{\alpha,2}$; K is an overall transport parameter.

For ideal gases, the corresponding entropy generation rate (9.29) can be written in the equivalent forms³

$$\dot{S}_{gen} = -\dot{n}_\alpha \bar{R} \ln \frac{p_{\alpha,2}}{p_{\alpha,1}} = -\dot{n}_\alpha \bar{R} \ln \left[1 - \frac{\dot{n}_\alpha}{K p_{\alpha,1}} \right] = \dot{n}_\alpha \bar{R} \ln \left[1 + \frac{\dot{n}_\alpha}{K p_{\alpha,2}} \right] . \tag{26.22}$$

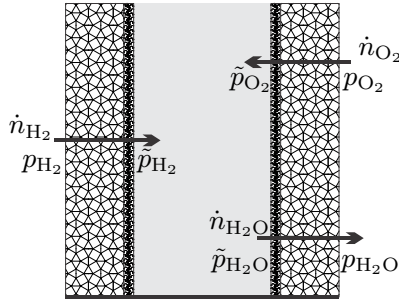


Fig. 26.6 Pressures in a fuel cell

The relevant mole flows and pressures for a hydrogen fuel cell are depicted in Fig. 26.6, where p_α denotes the pressures in the gas channels, and \tilde{p}_α denotes the pressures at the catalyst layers. Note that hydrogen and oxygen flow from the channels to the catalyst layer, while water flows in the opposite direction. The mole flows are related to current as

³ Check the differences between these forms carefully!

$$\begin{aligned}
 \dot{n}_{\text{H}_2} &= \frac{I}{2F} = K_{\text{H}_2} (p_{\text{H}_2} - \tilde{p}_{\text{H}_2}) , \\
 \dot{n}_{\text{O}_2} &= \frac{I}{4F} = K_{\text{O}_2} (p_{\text{O}_2} - \tilde{p}_{\text{O}_2}) , \\
 \dot{n}_{\text{H}_2\text{O}} &= \frac{I}{2F} = K_{\text{H}_2\text{O}} (\tilde{p}_{\text{H}_2\text{O}} - p_{\text{H}_2\text{O}}) .
 \end{aligned} \tag{26.23}$$

Thus, the respective entropy generation rates for the flows are

$$\begin{aligned}
 \dot{S}_{gen}^{\text{H}_2} &= -\frac{I}{2F} \bar{R} \ln \left[1 - \frac{I}{I_{\text{H}_2}} \right] , \\
 \dot{S}_{gen}^{\text{O}_2} &= -\frac{I}{4F} \bar{R} \ln \left[1 - \frac{I}{I_{\text{O}_2}} \right] , \\
 \dot{S}_{gen}^{\text{H}_2\text{O}} &= \frac{I}{2F} \bar{R} \ln \left[1 + \frac{I}{I_{\text{H}_2\text{O}}} \right] .
 \end{aligned} \tag{26.24}$$

For compact notation we used the abbreviation $I_\alpha = 2FK_\alpha p_\alpha / |\gamma_\alpha|$ for the so-called limiting currents. Note that all pressures in these are taken in the supply channels. The different forms of the expressions are due the fact that H_2 and O_2 are entering the device, while the water leaves; all three expressions are positive.

In the fuel cell literature, one sometimes finds these contributions to loss, or overpotential, subsumed into just one expression of the form

$$\dot{S}_{gen}^{\text{mass}} = -IB \ln \left[1 - \frac{I}{I_{\text{limit}}} \right] , \tag{26.25}$$

where B and I_{limit} are suitable parameters that describe the overall mass transfer losses. With this, the fuel cell potential (26.30) assumes the form

$$V = -\frac{\Delta \bar{g}_R(T, p_\alpha)}{2F} - BT \ln \left[1 - \frac{I}{I_{\text{limit}}} \right]^{-1} - \left[\frac{T \dot{S}_{gen}}{I} \right]_{\text{other}} . \tag{26.26}$$

Here, the last term refers to other contributions to entropy generation which will be discussed below.

In acidic fuel cells, water is produced at the cathode, and must be removed. In low temperature fuel cells the produced water is liquid, and might clog the pores of the gas diffusion layer, and even the gas channels. This reduces the transport parameter K and the limiting current I_{limit} . The air flow that provides the oxygen must be dry enough, so that the product water can evaporate into the exhaust. The use of excess air increases the water intake, and also guarantees sufficient oxygen pressures everywhere (see Nernst equation).

It is worth noting that the Nernst equation and the entropy generation terms for transport can be combined to give the fuel cell potential as⁴

⁴ This simple exercise is left to the reader.

$$V = -\frac{\Delta\bar{g}_R(T, \tilde{p}_\alpha)}{2F} - \left[\frac{T\dot{S}_{gen}}{I} \right]_{\text{other}} \quad (26.27)$$

This form of the equation shows that it is really the pressures \tilde{p}_α at the catalyst layers that are important. These however cannot be controlled, rather they depend on the pressures p_α in the gas channels and the current I as expressed in (26.23). This dependence is explicit in the form (26.26), which therefore must be used.

26.6 Resistance Losses

The ions travelling through the electrolyte between anode and cathode, and the electrons forming the electrical current that provides electrical power, experience resistance in the media they move in. The overall internal resistance of the fuel cell is denoted by R_i .

Electrical resistance is an irreversible process, and we proceed by determining the corresponding entropy generation, for a resistor at steady state. The resistor consumes work in form of electrical power $\dot{W} = -VI = -R_i I^2$, where I is the current and V is the voltage. The temperature of the resistor is T , and first and second law reduce to

$$0 = \dot{Q} - \dot{W} \quad , \quad -\frac{\dot{Q}}{T} = \dot{S}_{gen} \geq 0 \quad , \quad (26.28)$$

respectively. As done often before, first and second law are combined by eliminating the heat, which here gives⁵

$$\dot{S}_{gen} = -\frac{\dot{Q}}{T} = -\frac{\dot{W}}{T} = \frac{VI}{T} = \frac{R_i I^2}{T} \geq 0 \quad . \quad (26.29)$$

Electrical resistance produces entropy by downgrading electrical work to heat.

Thus, the voltage (26.8) of a fuel cell with resistance R_i is

$$V = -\frac{\Delta\bar{g}_R(T, p_\alpha)}{2F} - R_i I - BT \ln \left[1 - \frac{I}{I_{\text{limit}}} \right]^{-1} - \left[\frac{T\dot{S}_{gen}}{I} \right]_{\text{other}} \quad , \quad (26.30)$$

where the last term refers to other contributions to entropy generation.

In PEM fuel cells, a particular contribution to resistance loss is the drying-out of the membrane. The protons travelling from anode to cathode drag some water along, and this water is removed together with the product water. Thus, the membrane becomes somewhat dryer at the anode, and this reduces its conductivity, i.e., increases the membrane resistance. A common method to

⁵ Also here, the entropy generation can be considered as the product of a force (the potential V) and a flux (the current I). The linear relation between flux and force, $I = V/R$, guarantees positive entropy generation.

deal with this problem is to moisturize the incoming hydrogen fuel, so that new water is available at the anode.

26.7 Activation Overpotential

The third main cause for overpotential in fuel cells is activation loss. This irreversible effect is related to finite reaction rates and activation barriers at the reaction sites. The following discussion is based in part on the ideas discussed in Sec. 24.

At interfaces between different substances one observes electric potentials, due to different charge distribution at the interface. Figure 26.7 shows schematically the electric double layers that result at the interfaces between catalyst layers and electrolyte at anode and cathode in a fuel cell. For the sake of simplicity, the electrolyte at the interface is assumed to be electrically neutral.

The upper part of the figure shows anode and cathode potentials at open circuit, denoted as $V_{a,0}$ and $V_{c,0}$, with respect to an arbitrary reference, chosen such that the anode potential is negative and the cathode potential is positive. The overall cell potential at open circuit is $V_0 = V_{c,0} - V_{a,0}$.

The lower part of the figure sketches the conditions at closed circuit: a current flows and negative charges are removed from the anode, which becomes less negative, $V_a - V_{a,0} > 0$. On the other side, the additional electrons weaken the cathode potential, $V_c - V_{c,0} < 0$.

Due to reactions, new electrons are produced constantly at the anode, and consumed at the cathode. When the current is low, the electrons withdrawn are replaced through reactions, and the resulting change in the potentials is small. When the current is large, at the anode electrons are not replaced fast enough by reactions, and at the cathodes electrons are not consumed fast enough, so that the absolute values of the potentials drop. Thus, the overall potential of the cell, $V = V_c - V_a$, depends on the rate of reactions relative to the current drawn.

The activation overpotentials for anode and cathode are defined as

$$\eta_a = V_a - V_{a,0} \quad , \quad \eta_c = V_{c,0} - V_c \quad , \quad (26.31)$$

so that they both are positive, and the total overpotential is

$$\eta = \eta_a + \eta_c = V_0 - V \quad . \quad (26.32)$$

From the above discussion follows that the activation overpotential η should be small for small current, and large for large current. We proceed to find the relation between overpotential η and current I .

The anode and cathode potentials are related to the Gibbs free energies of reaction at anode and cathode as

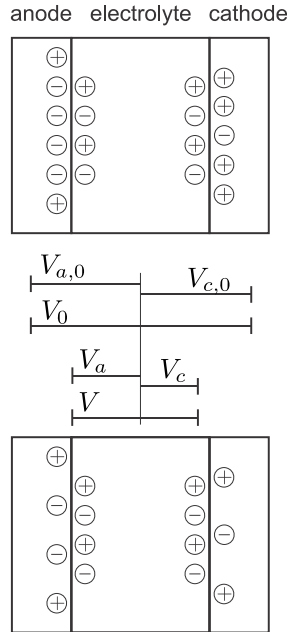


Fig. 26.7 Interface potentials and cell potential in a fuel cell. Top: open circuit. Bottom: closed circuit.

$$V_a = \frac{\Delta\bar{g}_a}{2F} = \frac{1}{2F} (-\bar{g}_{\text{H}_2} + 2\bar{g}_{\text{H}^+} + 2\bar{g}_{\text{e}^-}) , \quad (26.33)$$

$$V_c = -\frac{\Delta\bar{g}_c}{2F} = -\frac{1}{2F} \left(-\frac{1}{2}\bar{g}_{\text{O}_2} - 2\bar{g}_{\text{H}^+} - 2\bar{g}_{\text{e}^-} + \bar{g}_{\text{H}_2\text{O}} \right) . \quad (26.34)$$

The cell potential is, with $\Delta\bar{g}_R = \Delta\bar{g}_a + \Delta\bar{g}_c$,

$$V = V_c - V_a = -\frac{\Delta\bar{g}_R}{2F} = -\frac{1}{2F} \left(-\bar{g}_{\text{H}_2} - \frac{1}{2}\bar{g}_{\text{O}_2} + \bar{g}_{\text{H}_2\text{O}} \right) . \quad (26.35)$$

Adapting the results from Sec. 24.4, we write the entropy generation rate for the anode reaction as

$$\dot{S}_{gen,a} = -\frac{A}{T} \left[\bar{g}_f(V_a, T) - \bar{g}_b(V_a, T) + \bar{R}T \ln \prod X_\alpha^{\gamma_\alpha} \right] , \quad (26.36)$$

where $\bar{g}_f(V_a, T)$ and $\bar{g}_b(V_a, T)$ are activation barriers for the reactions, with $\Delta\bar{g}_a = \bar{g}_b - \bar{g}_f$. At open circuit the entropy generation vanishes, which implies the law of mass action in the form

$$\bar{g}_f(V_{a,0}, T) - \bar{g}_b(V_{a,0}, T) + \bar{R}T \ln \prod X_{\alpha,0}^{\gamma_\alpha} = 0 . \quad (26.37)$$

By subtracting this from the entropy generation, and multiplying with T/I we find the anode overpotential as

$$\begin{aligned} \eta_a &= \frac{T\dot{S}_{gen,a}}{I} \\ &= \frac{1}{2F} \left[\left(\bar{g}_f(V_{a,0}, T) - \bar{g}_f(V_a, T) + \bar{R}T \ln \prod_{\text{reactants}} \frac{X_\alpha^{|\gamma_\alpha|}}{X_{\alpha,0}^{|\gamma_\alpha|}} \right) \right. \\ &\quad \left. - \left(\bar{g}_b(V_{a,0}, T) - \bar{g}_b(V_a, T) + \bar{R}T \ln \prod_{\text{products}} \frac{X_\alpha^{\gamma_\alpha}}{X_{\alpha,0}^{\gamma_\alpha}} \right) \right]. \end{aligned} \quad (26.38)$$

The overpotential is larger the further the system is away from equilibrium. The activation barriers $\bar{g}_f(V_a, T)$ and $\bar{g}_b(V_a, T)$ depend on the current, and we proceed with their determination.

As a first step we note that the above equation (26.38) is satisfied by

$$\begin{aligned} \bar{g}_f(V_{a,0}, T) - \bar{g}_f(V_a, T) + \bar{R}T \ln \prod_{\text{reactants}} \frac{X_\alpha^{|\gamma_\alpha|}}{X_{\alpha,0}^{|\gamma_\alpha|}} &= 2F(1 - \beta_a)\eta_a, \\ \bar{g}_b(V_{a,0}, T) - \bar{g}_b(V_a, T) + \bar{R}T \ln \prod_{\text{products}} \frac{X_\alpha^{\gamma_\alpha}}{X_{\alpha,0}^{\gamma_\alpha}} &= -2F\beta_a\eta_a, \end{aligned} \quad (26.39)$$

for arbitrary coefficients β_a . For interpretation we can say that the parameter β_a distributes the overpotential η_a between the forward and the backward reactions. In principle, β_a could be a complicated function of current, temperature and other parameters, but experimental measurements show that it is a constant.

Reaction rates and current are related as

$$I = 2F\Lambda = 2F(r_f - r_b), \quad (26.40)$$

where r_f and r_b are the forward and backward reaction rates, respectively. From the results of Chapter 24 we can write the reaction rates as

$$\begin{aligned} r_f &= k_0 \exp \left[-\frac{\bar{g}_f(V_a, T)}{\bar{R}T} \right] \prod_{\text{reactants}} X_\alpha^{|\gamma_\alpha|}, \\ r_b &= k_0 \exp \left[-\frac{\bar{g}_b(V_a, T)}{\bar{R}T} \right] \prod_{\text{products}} X_\alpha^{\gamma_\alpha}, \end{aligned} \quad (26.41)$$

where k_0 is a rate constant. We introduce the exchange current I_0 as the current associated with the number of reactions taking place at open circuit in either direction; recall that forward and backward reaction rates are equal at open circuit. For the anode

$$I_{0,a} = 2F r_f (V_{a,0}) = 2F r_b (V_{a,0}) , \quad (26.42)$$

or, in more detail,

$$\begin{aligned} I_{0,a} &= 2F k_0 \exp \left[-\frac{\bar{g}_f (V_{a,0}, T)}{RT} \right] \prod_{\text{reactants}} X_{\alpha,0}^{|\gamma_\alpha|} \\ &= 2F k_0 \exp \left[-\frac{\bar{g}_b (V_{a,0}, T)}{RT} \right] \prod_{\text{products}} X_{\alpha,0}^{\gamma_\alpha} . \end{aligned} \quad (26.43)$$

With this, we can write the total current as

$$\begin{aligned} I &= I_{0,a} \frac{2F [r_f - r_b]}{I_{0,a}} \\ &= I_{0,a} \left(\exp \left[\frac{\bar{g}_f (V_{a,0}, T) - \bar{g}_f (V_a, T)}{RT} + \ln \prod_{\text{reactants}} \frac{X_\alpha^{|\gamma_\alpha|}}{X_{\alpha,0}^{|\gamma_\alpha|}} \right] \right. \\ &\quad \left. - \exp \left[\frac{\bar{g}_b (V_{a,0}, T) - \bar{g}_b (V_a, T)}{RT} + \ln \prod_{\text{products}} \frac{X_\alpha^{\gamma_\alpha}}{X_{\alpha,0}^{\gamma_\alpha}} \right] \right) . \end{aligned} \quad (26.44)$$

The expressions in the exponentials are just those that occur in the 2nd law expression for the overpotential (26.38). Replacing them with (26.39) finally leads to the desired relation between current and overpotential, the Butler-Volmer equation (Max Volmer, 1885-1965; John Butler, 1899-1977):

$$I = I_{0,a} \left(\exp \left[\frac{2F (1 - \beta_a) \eta_a}{RT} \right] - \exp \left[-\frac{2F \beta_a \eta_a}{RT} \right] \right) . \quad (26.45)$$

Due to the sign conventions used here, the Butler-Volmer equation for the cathode is obtained simply by switching signs, as

$$I = I_{0,c} \left(\exp \left[\frac{2F \beta_c \eta_c}{RT} \right] - \exp \left[-\frac{2F (1 - \beta_c) \eta_c}{RT} \right] \right) . \quad (26.46)$$

For large overpotentials the exponential with negative argument can be ignored against the exponential with positive argument; in this limit the Butler-Volmer equation reduces to the so-called Tafel equation (Julius Tafel, 1862-1918), e.g., for the anode,

$$\eta_a = \frac{\bar{R}T}{2F (1 - \beta_a)} \ln \frac{I}{I_{0,a}} \quad \text{for} \quad \frac{2F (1 - \beta_a) \eta_a}{\bar{R}T} \gg 1 . \quad (26.47)$$

Figure 26.8 shows the Butler-Volmer and the Tafel equation in a logarithmic plot (*Tafel plot*), that is overvoltage η as function of $\ln I$. The curves are plotted for a constant value for the parameter β . Both curves coincide at larger η , where the approximation (26.47) is valid. The overpotential can be

measured (not shown), and the resulting curve agrees with the prediction of the Butler-Volmer equation when β and I_0 are adjusted properly. Indeed, β and I_0 can be read of the experimental Tafel plot as slope and intercept as indicated in the figure.

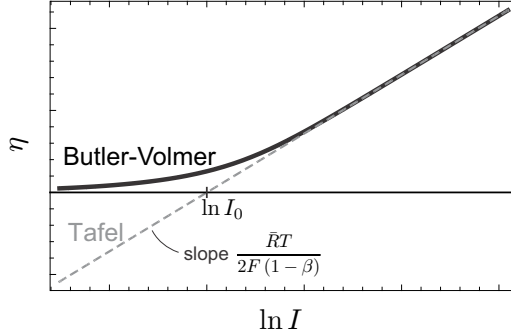


Fig. 26.8 Tafel plot: $\eta(\ln I)$ according to the Butler-Volmer equation (continuous line) and the Tafel equation (dashed). Both equations agree for large η .

According to the Butler-Volmer equation the activation overpotential will be smaller for large exchange currents I_0 . For an efficient fuel cell one must aim to make the exchange current large. According to (26.43), the exchange current depends on an activation energy and on temperature. It grows with temperature, so that activation losses are smaller for high temperature fuel cells. The activation barriers \bar{g}_f, \bar{g}_b depend strongly on the electrode material: good catalysts have low activation energies and thus low overpotential. For a hydrogen electrode at T_0 , the following data for the exchange current per unit area can be found in the literature:

$$\begin{aligned}
 \text{lead:} & \quad \hat{I}_0 = 2.5 \times 10^{-13} \frac{\text{A}}{\text{cm}^2}, \\
 \text{nickel:} & \quad \hat{I}_0 = 6 \times 10^{-6} \frac{\text{A}}{\text{cm}^2}, \\
 \text{platinum:} & \quad \hat{I}_0 = 5 \times 10^{-4} \frac{\text{A}}{\text{cm}^2}, \\
 \text{palladium:} & \quad \hat{I}_0 = 4 \times 10^{-3} \frac{\text{A}}{\text{cm}^2}.
 \end{aligned}$$

The data indicates that expensive catalysts must be used at low temperatures. The most common catalyst for low temperature fuel cells is platinum. No catalysts are required for high temperature fuel cells. The total exchange current of a fuel cell is proportional to the surface of the catalyst layer, $I_0 = \hat{I}_0 A_{\text{catalyst}}$. To reach sufficient catalyst area, the catalyst must be distributed well within the catalyst layer, e.g., as extremely small spheres.

In hydrogen fuel cells, typically the reaction at the anode is considerably slower than the reaction at the cathode. Then, the activation overpotential at the cathode is small and can be ignored against the anode overpotential.

We end the discussion with a short look on the activation energies for forward and backward reactions, for which the reaction rates can be written as

$$r_f = I_{0,a} \exp \left[\frac{2F(1-\beta)\eta_a}{RT} \right] , \quad r_b = I_{0,a} \exp \left[-\frac{2F\beta\eta_a}{RT} \right] . \quad (26.48)$$

These equations imply that the overpotential leads to a change in energy barriers and reaction rates. Figure 26.9 illustrates the influence of the overpotential on the energy landscape, similar to Fig. 24.2 and the discussion around it.

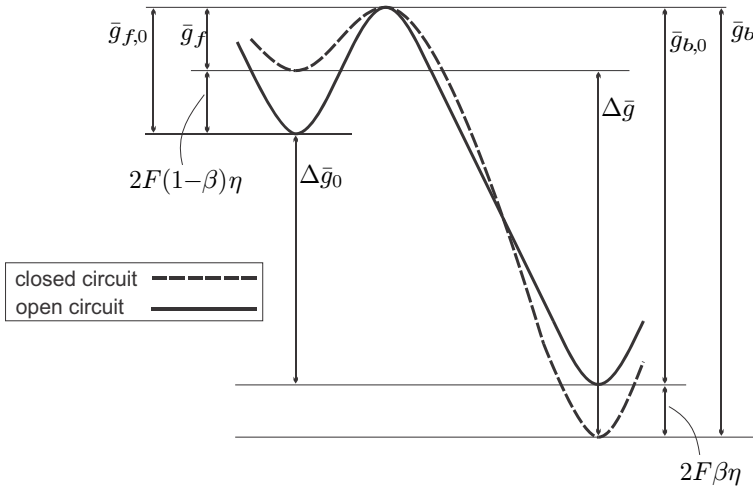


Fig. 26.9 Energy landscape for open circuit and closed circuit cell

26.8 Voltage/Current and Power/Current Diagrams

Summarizing the results of the last sections, the fuel cell potential is

$$V = -\frac{\Delta\bar{g}_R}{2F} - R_i I - BT \ln \left[1 - \frac{I}{I_{\text{limit}}} \right]^{-1} - \eta(I) , \quad (26.49)$$

where the first term is the open circuit potential, and the following three terms describe the irreversible losses due to resistance, mass transfer and activation. Figure 26.10 compares the actual potential (continuous) with the open circuit potential (grey), and also shows the individual losses, all in dimensionless quantities where the open circuit potential is unity.

The activation loss (short dashes) causes the sharp drop of the potential for small currents, it grows only slightly for larger currents. The resistance

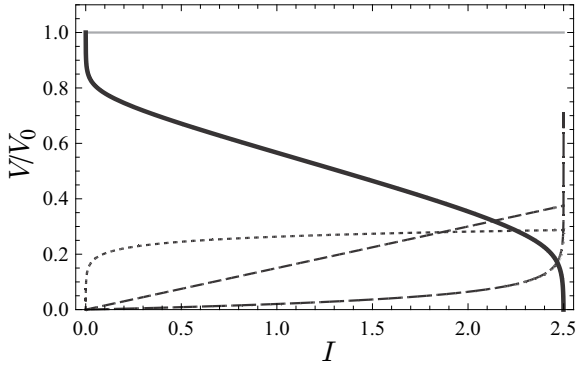


Fig. 26.10 Fuel cell potential (continuous), open circuit potential (grey), resistance loss (dashes), mass transfer loss (long dashes), activation loss (short dashes) as functions of current; $T/T_0 = 1$

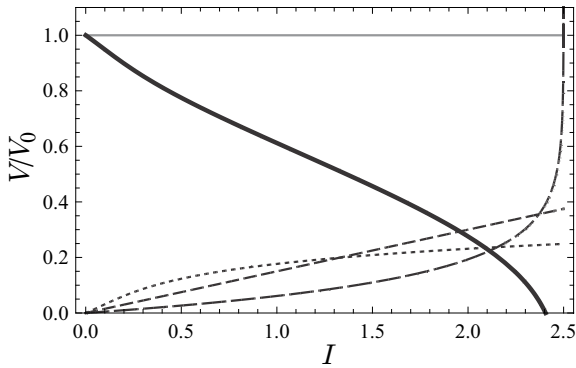


Fig. 26.11 Same as Fig. 26.10, but higher temperature; $T/T_0 = 3$

loss (dashes) grows linearly with current and causes the linear drop of the potential in the middle. The mass transfer loss (long dashes) is relatively small until the current approaches the limiting current which causes a sharp increase, and the sudden drop of the potential.

These curves agree qualitatively with curves found in the specialist literature on fuel cells. The relative contribution of the different losses depends on design and materials, and on temperature.

Figure 26.11 shows the same curves at a higher temperature. Now the activation losses are reduced, but the mass transfer losses are increased. It should be noted that low and high temperature fuel cells are fundamentally different in materials, physical processes and design, and thus this is only a qualitative comparison.

The power-current characteristic is shown in Fig. 26.12, based on the same data as the first voltage curve, Fig. 26.10. A reversible fuel cell would deliver the power $V_0 I$ (continuous), but due to the various losses, the power curve exhibits a maximum, and drops to zero at the limiting current. In order to minimize the losses, a fuel cell should operate at currents well left of the maximum, where the losses are relatively small. Note that the power loss is the difference between the actual power curve and the reversible curve, and grows non-linearly with current!

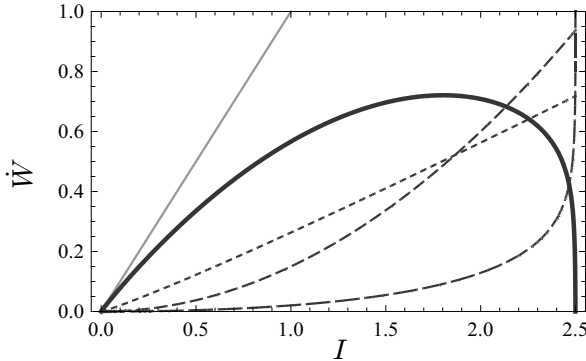


Fig. 26.12 Fuel cell power (continuous), reversible power (grey), resistance loss (dashes), mass transfer loss (long dashes), activation loss (short dashes)—all as function of current drawn

26.9 Crossover Losses

Even when the circuit is open, the observed potential lies below the open circuit potential (which describes reversible operation). The common explanation for this drop is the occurrence of electron crossover losses, due to electrons that find a path through the electrolyte and travel from anode to electrode without delivering electrical work. Thus, there is a certain number of net reactions taking place which do not contribute to the useful current I_{used} . The overall current $I = 2F\Lambda$, where Λ is the fuel consumption rate, can be split into the useful current and the crossover current I_{lost} , so that the voltage-current relation reads

$$V = -\frac{\Delta\bar{g}_R}{2F} - R_i (I_{\text{used}} + I_{\text{lost}}) - BT \ln \left[1 - \frac{I_{\text{used}} + I_{\text{lost}}}{I_{\text{limit}}} \right]^{-1} - \eta (I_{\text{used}} + I_{\text{lost}}) . \tag{26.50}$$

When plotted over the useful current for constant I_{lost} , the current scale is merely shifted, Fig. 26.13 shows an example.

Additional losses can occur due to fuel and oxidizer entering the electrolyte, and reacting directly, without flow of electrons involved. This does not affect

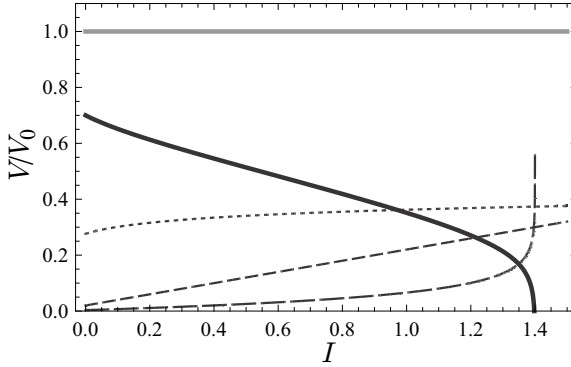


Fig. 26.13 Same as Fig. 26.10, but with crossover loss I_{loss}

the potential V of the fuel cell, nor the power drawn which still is $\dot{W} = VI$, but leads to additional heat developed by the fuel cell, and additional fuel consumption.

If the reaction rate of these reactions is Λ_c , the corresponding heat to be removed from the fuel cell is $\dot{Q}_c = -\Lambda_c \Delta \bar{h}_R$. This heat, if unused, leads to external entropy generation, and waste of fuel.

The work potential of the fuel consumed in crossover is $-\Lambda_c \Delta \bar{g}_R$, and, since this potential is not used, this is just the entropy generated in fuel crossover, $T \dot{S}_{gen}^c = -\Lambda_c \Delta \bar{g}_R$. The relation between power and entropy generation is $\dot{W} = -\Lambda \Delta \bar{g}_R - T \dot{S}_{gen}$ where Λ counts all reactions, i.e., the fuel consumption. Accounting explicitly for the loss due to crossover, we have

$$\dot{W}_{FC} = -\Lambda \Delta \bar{g}_R + \Lambda_c \Delta \bar{g}_R - T \dot{S}_{gen} = -\Lambda_I \Delta \bar{g}_R - T \dot{S}_{gen}^I, \quad (26.51)$$

where $\Lambda_I = \Lambda - \Lambda_c = \frac{I}{2F}$ is the reaction rate for electrochemical reactions. Moreover, $T \dot{S}_{gen}^I$ denotes the power loss due to all mechanisms discussed above, excluding crossover loss. Thus, the expressions for fuel cell work of the previous sections remain valid. Fuel crossover does not affect the voltage-current curve, but leads to increased fuel consumption, and increased heat transfer from the cell.

The influence of crossover is best seen in the second law efficiency for the fuel cell. The reversible work available from the fuel is $\dot{W}_{rev} = -\Lambda \Delta \bar{g}_R$ where the reaction rate Λ measures the amount of fuel used. With $\Lambda_I = \Lambda - \Lambda_c$ the second law efficiency becomes

$$\eta_{II} = \frac{\dot{W}_{FC}}{\dot{W}_{rev}} = 1 - \frac{\Lambda_c}{\Lambda_I + \Lambda_c} - \frac{T \dot{S}_{gen}}{(\Lambda_I + \Lambda_c) (-\Delta \bar{g}_R)}. \quad (26.52)$$

26.10 Electrolyzers

In fuel cells, hydrogen and oxygen combine to produce electrical energy and water. In electrolyzers, the opposite takes place: electrical energy is used to split water into hydrogen and oxygen. Figure 26.14 shows the basic reactions taking place, and indicates the flows of hydrogen, oxygen, water, protons, and electrons.

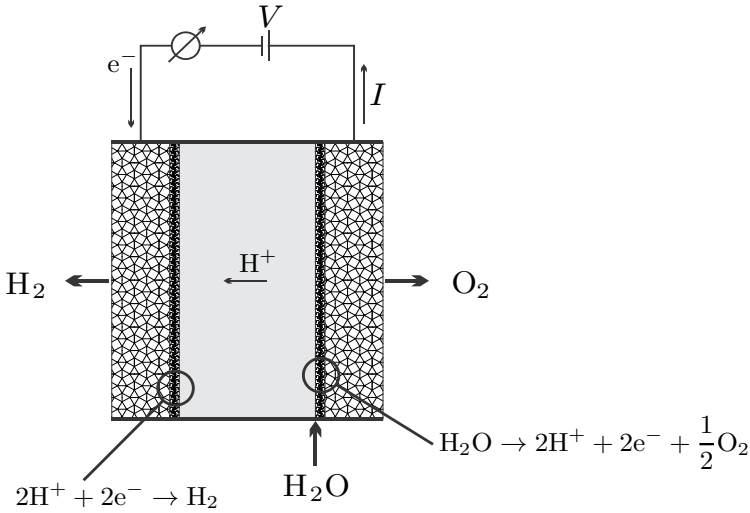


Fig. 26.14 Reactions and flows in an electrolyzer

The power consumption of the electrolyzer is $\dot{W}_E = -V_E I$ and the amount of hydrogen produced is equal to the reaction rate $\Lambda = I/2F$. Thus, the work required for the production per molar of hydrogen, w_{H_2} , is directly proportional to the electrolyzer potential,

$$w_{\text{H}_2} = \frac{\dot{W}_E}{\Lambda} = -2FV_E. \quad (26.53)$$

Since all flows are just in opposite direction as in a fuel cell, the potential and power consumption for an electrolyzer follow from the equations for fuel cells simply by inverting the sign of the electrical current. Then, from (26.49), the electrolyzer potential becomes

$$V_E = -\frac{\Delta\bar{g}_R}{2F} - R_i(-I) - BT \ln \left[1 - \frac{-I}{I_{\text{limit}}} \right]^{-1} - \eta(-I), \quad (26.54)$$

where $\eta(-I)$ solves the Butler-Volmer equation for negative current,

$$-I = I_0 \left[\exp \left[\frac{2F(1 - \beta)\eta}{\bar{R}T} \right] - \exp \left[-\frac{2F\beta\eta}{\bar{R}T} \right] \right] ; \tag{26.55}$$

obviously, $\eta(-I) = -\eta_E(I)$ must be negative.

With the positive activation potential η_E , the electrolyzer equations become

$$V_E = -\frac{\Delta\bar{g}_R}{2F} + R_i I + BT \ln \left[1 + \frac{I}{I_{\text{limit}}} \right] + \eta_E , \tag{26.56}$$

$$I = I_0 \left[\exp \left[\frac{2F\beta\eta_E}{\bar{R}T} \right] - \exp \left[-\frac{2F(1 - \beta)\eta_E}{\bar{R}T} \right] \right] . \tag{26.57}$$

Irreversible processes due to internal resistance, mass transfer, and activation lead to an increase of the potential above the open circuit potential $V_0 = -\frac{\Delta\bar{g}_R}{2F}$. The proper second-law efficiency measure for an electrolyzer is

$$\eta_{II} = \frac{V_0}{V_E} \leq 1 . \tag{26.58}$$

Figure 26.15 compares the voltage-current curves for fuel cell and electrolyzer to the open circuit potential. The gap between the curves is the loss to irreversible processes.

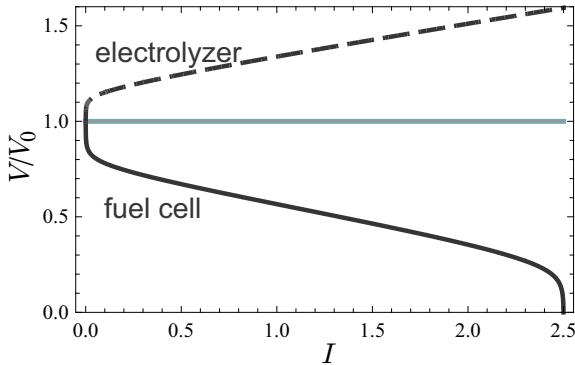


Fig. 26.15 Voltage-current curves for fuel cell and electrolyzer

26.11 Hydrogen

A common method to produce hydrogen is steam methane reforming, in which hydrogen (H_2) is split from natural gas (that is mainly methane, CH_4) according to the overall reaction $CH_4 + 2H_2O \leftrightarrow 4H_2 + CO_2$. Larger quantities of H_2 are produced this way for NH_3 production (see Sec. 23.10). This process generates CO_2 and thus is not carbon neutral. If the natural gas is used in

a combined cycle power plant with thermal efficiency of 60% (Sec. 13.6), there will be less CO_2 produced per kWh of electricity than if H_2 from steam methane reforming is used in a fuel cell.

By means of electrolyzers, hydrogen can be produced from any primary source of electrical power, including carbon neutral power sources like nuclear, solar, wind, or tidal. As opposed to electricity, hydrogen can be stored and distributed in pipelines and tanks, and therefore offers a means to store power produced from intermittent sources (solar, wind, tidal).

The stored hydrogen can be reconverted into electricity either in traditional combustion systems (e.g. combined cycle power plants, Atkinson cycle), or in fuel cells. The latter offer an elegant and efficient means to use power produced by stationary non-carbon power plants (solar, wind, ...) for transportation (cars, trucks, busses, trains, ...). The use of hydrogen produced by carbon neutral energy sources could play a role in the future energy system, which must aim to reduce the emission of greenhouse gases, including carbon dioxide.

Due to irreversibilities, only a portion of the energy fed into the electrolyzer is retrieved from the fuel cell. Moreover, one needs to account for the efficiency of processes required to store and distribute the hydrogen. Indeed, at normal conditions hydrogen is a gas which, due to its low molar mass, assumes a relatively large specific volume. In particular for use as transportation fuel, the hydrogen needs to be compacted, either by compression of the gas, or by liquefaction. The (irreversible) processes involved can be described by a storage and distribution efficiency measure η_{SD}^{II} .

With the second law efficiencies for electrolyzer, storage and distribution, and fuel cell, the ratio between the power provided by the fuel cell, \dot{W}_{FC} , and the power \dot{W}_E which was consumed to produce the hydrogen in the electrolyzer, is

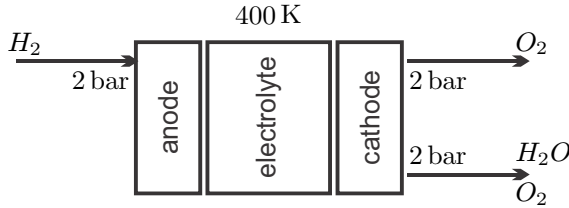
$$\frac{\dot{W}_{FC}}{\dot{W}_E} = \eta_{FC}^{\text{II}} \eta_{SD}^{\text{II}} \eta_E^{\text{II}}. \quad (26.59)$$

Typical values for these efficiencies are $\eta_{FC}^{\text{II}} = 0.6$, $\eta_{SD}^{\text{II}} = 0.75$, $\eta_E^{\text{II}} = 0.6$, so that only 27% of the energy provided at the source is finally recovered. Doubtless, new materials and better designs will lead to efficiency improvements in the future. Meanwhile, other storage concepts might have higher efficiencies, e.g., batteries or pumped hydro.

Problems

26.1. Fuel Cell Potential

Compute the maximum voltage (reversible operation) for the fuel cell depicted below under the assumption that the oxygen supplied is five times the stoichiometric amount. Assume isothermal operation and assume that the water leaves as vapor.



26.2. Fuel Cell Potential and Power

We can write the fuel cell voltage as $V = V_0 - V_R - V_{tr} - \eta$, where V_0 is the open circuit potential, $V_R = \mathcal{R}I$ are the ohmic losses due to the internal resistance \mathcal{R} of the fuel cell, and $V_{tr} = -BT \ln(1 - I/I_{limit})$ is the potential drop due to mass transfer loss. Moreover the activation overpotential η is related to the current I through the Butler-Volmer equation

$$I = I_0 \left\{ \exp \left[\frac{2F(1 - \beta)\eta}{R_u T} \right] - \exp \left[-\frac{2F\beta\eta}{R_u T} \right] \right\},$$

where the exchange current is modelled as (constant factor k_I , activation energy E_a)

$$I_0 = k_I T \exp \left[-\frac{E_a}{R_u T} \right].$$

1. Introduce dimensionless quantities, and show that the dimensionless voltage can be written as

$$v = 1 - \rho i - \gamma \hat{T} \ln [1 - \varepsilon i] - \hat{\eta}$$

with

$$i = \hat{T} \exp \left[-\frac{e_a}{\hat{T}} \right] \left\{ \exp \left[\frac{\alpha(1 - \beta)\hat{\eta}}{\hat{T}} \right] - \exp \left[-\frac{\alpha\beta\hat{\eta}}{\hat{T}} \right] \right\},$$

Identify the dimensionless quantities that appear in the above.

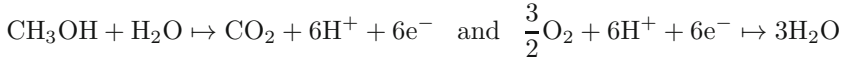
2. Chose $\alpha = 95$, $\beta = 0.6$, $\gamma = 0.04$, $\rho = 0.15$, $\varepsilon = 0.4$, $e_a = 10$, and plot dimensionless voltage v and power $w = vi$ for some values of the dimensionless temperature \hat{T} between 1 and 5. Also plot the individual voltage losses into the same diagram.

26.3. Electrolyzer

An electrolyzer can be considered as an “inverted fuel cell”: it consumes electric power and produces hydrogen and oxygen gases. For the following, ignore mass transfer contributions. Obviously, the current in the electrolyzer flows in the opposite direction: replace I by $-I$ in the fuel cell equations of the previous problem. Show that now resistance and activation increase the fuel cell potential. Use the same constants as for the fuel cell, and plot the electrolyzer potential over the current, and also the power consumed as a function of current.

26.4. Direct Methanol Fuel Cell

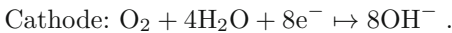
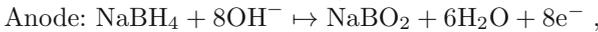
In a direct methanol fuel cell, liquid methanol CH_3OH reacts with oxygen to form water and carbon dioxide. The half-reactions at anode and cathode follow the equations



Determine the open circuit voltage at 330K. Assume methanol is an incompressible liquid with constant specific heat $\bar{c}_{\text{CH}_3\text{OH}} = 0.082 \frac{\text{kJ}}{\text{mol K}}$.

26.5. Borohydride Fuel Cell

The reactions in a direct borohydride fuel follow the equations



Determine the open circuit voltage at standard conditions (Remark: Actual devices operate at elevated temperatures). Assume that all participating components enter or leave in separate streams. Use the following data:

NaBH_4 : $\bar{h}_f^0 = -192 \frac{\text{kJ}}{\text{mol}}$, $\bar{s}_f^0 = 101 \frac{\text{J}}{\text{mol K}}$; NaBO_2 : $\bar{h}_f^0 = -960 \frac{\text{kJ}}{\text{mol}}$, $\bar{s}_f^0 = 83 \frac{\text{J}}{\text{mol K}}$.

26.6. Electrolyzer

Compute the voltage of a reversible electrolyzer that splits liquid water into hydrogen and oxygen. Assume that all incoming and outgoing streams are at reference pressure $p_0 = 1 \text{ atm}$ and have a temperature of 360 K.

26.7. Direct Carbon Fuel Cell

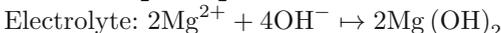
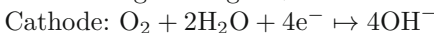
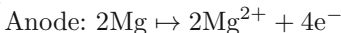
The anode and cathode reactions in a direct carbon fuel cell follow the equations



Determine the open circuit voltage at 900 K, which is the typical operating temperature of actual DCFC's. Assume carbon (graphite) is a incompressible substance with specific heat $c_p = 0.71 \frac{\text{J}}{\text{kg K}}$.

26.8. Magnesium Fuel Cell

The reactions in a Magnesium fuel cell with salt water electrolyte follow the equations

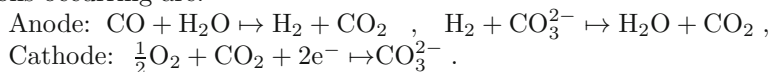


Determine the open circuit voltage at standard conditions (Remark: Actual devices operate at elevated temperatures).

26.9. Molten Carbonate Fuel Cell

Molton carbonate fuel cells (MCFC) employ a mixture of salt and molten carbonate as electrolyte, and operate at temperatures around 900 K.

MCFC can work with carbon monoxide (CO) as fuel. Then the anode reaction occurs in two steps, first the water gas shift reaction, followed by reaction of the generated hydrogen with the carbonate ion, CO_3^{2-} . The reactions occurring are:



1. Make a sketch of a fuel cell, where you indicate the relevant flows.
2. Determine the open circuit voltage at standard conditions and at 900 K.